



OPEN

Genetic engineering of *Pseudomonas chlororaphis* Lzh-T5 to enhance production of trans-2,3-dihydro-3-hydroxyanthranilic acid

Kaiquan Liu^{1,4}, Ling Li^{1,2,4}✉, Wentao Yao¹, Wei Wang³✉, Yujie Huang², Ruiming Wang¹ & Piwu Li¹

Trans-2,3-dihydro-3-hydroxyanthranilic acid (DHHA) is a cyclic β -amino acid used for the synthesis of non-natural peptides and chiral materials. And it is an intermediate product of phenazine production in *Pseudomonas* spp. Lzh-T5 is a *P. chlororaphis* strain isolated from tomato rhizosphere found in China. It can synthesize three antifungal phenazine compounds. Disruption the *phzF* gene of *P. chlororaphis* Lzh-T5 results in DHHA accumulation. Several strategies were used to improve production of DHHA: enhancing the shikimate pathway by overexpression, knocking out negative regulatory genes, and adding metal ions to the medium. In this study, three regulatory genes (*psrA*, *pykF*, and *rpeA*) were disrupted in the genome of *P. chlororaphis* Lzh-T5, yielding 5.52 g/L of DHHA. When six key genes selected from the shikimate, pentose phosphate, and gluconeogenesis pathways were overexpressed, the yield of DHHA increased to 7.89 g/L. Lastly, a different concentration of Fe^{3+} was added to the medium for DHHA fermentation. This genetically engineered strain increased the DHHA production to 10.45 g/L. According to our result, *P. chlororaphis* Lzh-T5 could be modified as a microbial factory to produce DHHA. This study laid a good foundation for the future industrial production and application of DHHA.

Trans 2,3-dihydro-3-hydroxyanthranilic acid (DHHA) can be used in cycloaddition reactions as an enantiomerically pure building block, for biosynthesis of unnatural peptides, and for preparation of various useful intermediate acid derivatives of benzoic acid, such as 3-hydroxyanthranilic acid and anthranilic acid, which are important aromatic compounds^{1–4}. These compounds are widely used in chemicals, food, cosmetics, and pharmaceuticals. In the current market, production of aromatic compounds relies heavily on direct extraction from plants or petroleum-derived chemical processes. The demand for establishing new sustainable sources and renewable aromatics has increased rapidly in recent years. The sustainable production of aromatics has drawn great interest^{5–8}. Microbial bioproduction using abundant feedstocks is a highly promising alternative⁸.

In recent years, the use of renewable resources to produce chemicals and fuels has attracted the attention of researchers^{9–11}. Different than other aromatic compounds, DHHA can be synthesized in microorganisms. McCormick et al. first isolated DHHA from the fermentation broth of *Streptomyces aureofaciens* S-652 and Meade et al. obtained an *S. aureofaciens* strain which had a production of 8 g/L of DHHA after 120 h of fermentation^{3,12}. According to previous research by Mavrodi et al., benzoate was converted to 2-amino-4-deoxycholic acid (ADIC) by PhzE, and then converted by PhzD to DHHA, in certain *Pseudomonas* strains. DHHA is an important intermediate of the phenazine biosynthesis of *Pseudomonas* spp (Fig. 1)^{13,14}.

¹State Key Laboratory of Biobased Material and Green Papermaking (LBMP), School of Bioengineering, Qilu University of Technology (Shandong Academy of Sciences), Jinan 250353, Shandong, People's Republic of China. ²Shandong Provincial Key Laboratory of Applied Microbiology, Ecology Institute, Qilu University of Technology (Shandong Academy of Sciences), Jinan 250103, People's Republic of China. ³State Key Laboratory of Microbial Metabolism, School of Life Sciences and Biotechnology, Shanghai Jiao Tong University, Shanghai 200240, People's Republic of China. ⁴These authors contributed equally: Kaiquan Liu and Ling Li. ✉email: liling33802400@qlu.edu.cn; weiwang100@sjtu.edu.cn

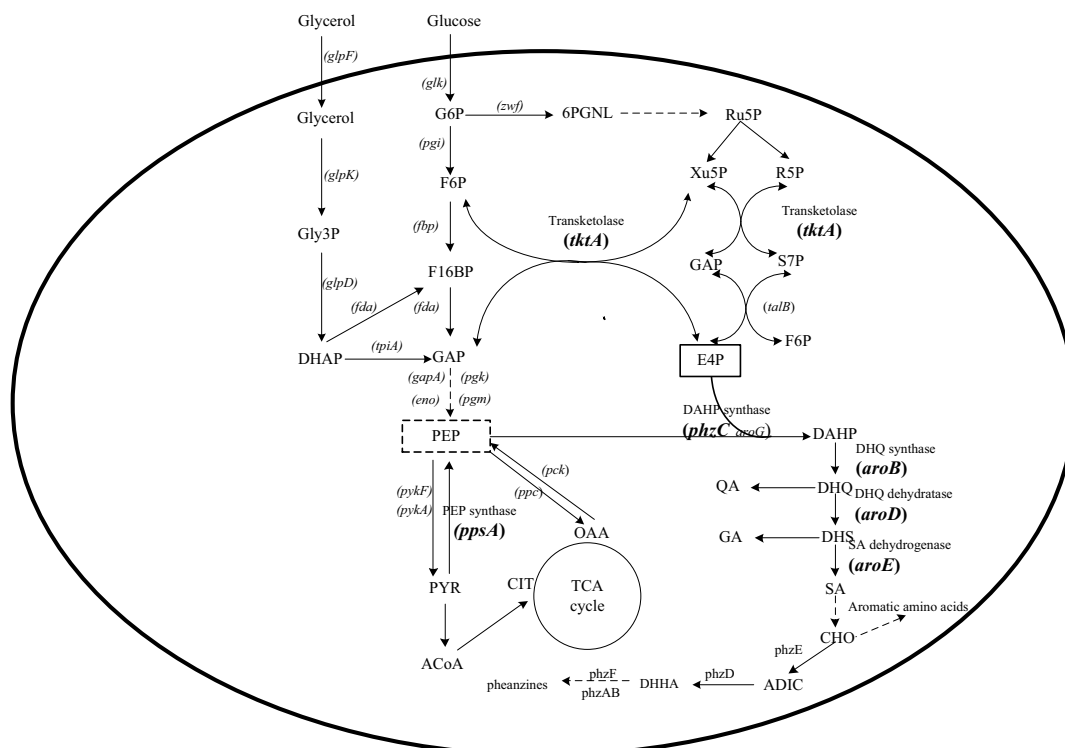


Figure 1. Central carbon metabolism related to the biosynthesis of phenazines in *P. chlororaphis* Lzh-T5. The enzymes: *pgi*, phosphoglucose isomerase; *glk*, glucokinase; *eno*, enolase; *gapA*, glyceraldehyde 3-phosphate dehydrogenase; *glpK*, glycerol kinase; *glpF*, glycerol facilitator; *fda*, fructose-1,6-P2 aldolase; *glpD*, glycerol-3-P dehydrogenase; *fbp*, fructose 1,6-bisphosphatase; *tpiA*, triosephosphate isomerase; *talB*, transaldolase; *zwf*, G6P dehydrogenase; *pck*, PEP carboxykinase; *ppc*, PEP carboxylase; *pgm*, phosphoglyceromutase; *pgk*, phosphoglycerate kinase; *phzF*, asparagine synthase. DHAP dihydroxyacetone phosphate; Gly3P Glycerol 3-phosphate; G6P glucose 6-phosphate; F16BP fructose 1,6-bisphosphate; GAP glyceraldehyde 3-phosphate; F6P fructose 6-phosphate; 6PGNL 6-phosphogluconolactone; R5P ribose 5-phosphate; Ru5P ribulose 5-phosphate; S7P sedoheptulose 7-phosphate; Xu5P xylulose 5-phosphate; PEP phosphoenolpyruvate; E4P erythrose 4-phosphate; ACoA acetyl-coenzyme A; PYR pyruvate; OAA oxaloacetate; CIT citrate; DHQ 3-dehydroquinic acid; DAHP 3-deoxy-Darabinoheptulosonate7-phosphate; QA quinic acid; DHS 3-dehydroshikimic acid; SA shikimic acid; GA gallic acid; CHO chorismate.

Lzh-T5 is a *P. chlororaphis* strain isolated from the tomato rhizosphere located in China. It has a phenazine biosynthesis cluster *phzABCDEFG*, and could produce phenazine-1-carboxylic acid (PCA) and other phenazine derivatives¹⁵. In this study, *phzF* of *P. chlororaphis* Lzh-T5 was disrupted causing DHHA accumulation. Three negative regulatory genes (*pykF*, *psrA*, and *rpeA*) were stepwise disrupted in *P. chlororaphis* Lzh-T5. The yield of DHHA increased from 2.15g/L to 5.52 g/L. To improve DHHA production, key genes were overexpressed by BglBrick vectors from the shikimate, pentose phosphate, and gluconeogenesis pathways of Lzh-T5, obtaining 7.89 g/L DHHA. The effect of Fe³⁺ on DHHA production was investigated. A final DHHA yield of 10.45 g/L was obtained.

Methods

Microorganisms, growth conditions, and plasmids. All plasmids, primers, and microorganisms are listed in Table 1 and Supplementary Material 1: Table S1. All *Escherichia coli* strains were cultured in LB medium at 37 °C, and all *P. chlororaphis* strains were cultured in KB medium at 30 °C. Kanamycin and Ampicillin were used. All details are detailed in our previous research¹⁶.

DNA manipulation. A no-scar deletion method was used in the genome of *P. chlororaphis* Lzh-T5 and its derivative strain. In order to create LDA-1 by the interruption of *phzF* in Lzh-T5, two pairs of primers (*phzF*-A (EcoRI)-*phzF*-B and *phzF*-C-*phzF*-D (XbaI)) were designed. Upstream (740 bp) and downstream (793 bp) of *phzF* were first amplified by PCR. A 1515 bp fragment fusion was amplified by overlap PCR. The fusion fragment was constructed into pK18mobsacB, creating the recombinant plasmid pK18-*phzF*.

The pK18-*phzF* plasmid was transferred to *E. coli* S17-1 (λpir) by heat shock transformation. Then biparental mating between *E. coli* S17-1 and *P. chlororaphis* Lzh-T5 generated the mutant LDA-1 strain. Single-crossover and double-crossover clones were selected stepwise. To ensure accuracy, PCR analysis and sequencing were used to confirm the deletion. Detailed steps are listed in our previous research¹⁶. Similarly, *rpeA*, *pykF*, and *psrA* were disrupted in their corresponding strains.

Strains and plasmids	Relevant gene type	Reference/source
Strains		
DH5 α	<i>E. coli</i> F ⁻ Φ 80lacZ Δ M15 Δ (lacZYA-argF) U169 recA1 endA1 hsdR17 (r _k ⁻ m _k ⁻) <i>phoA supE44 thi</i> ⁻¹ <i>gyrA96 relA1</i>	Lab stock
<i>E. coli</i> S17-1(λ pir)	res ⁻ pro mod ⁺ integrated copy of RP4, mob ⁺ , used for incorporating constructs into <i>P. chlororaphis</i>	Lab stock
Lzh-T5	wild-type strain of <i>P. chlororaphis</i> Lzh-T5	Lab stock
LDA-1	<i>phzF</i> gene deletion of <i>P. chlororaphis</i> Lzh-T5	This work
LDA-2	<i>pykF</i> gene deletion of <i>P. chlororaphis</i> LDA-1	This work
LDA-3	<i>psrA</i> gene deletion of <i>P. chlororaphis</i> LDA-2	This work
LDA-4	<i>rpeA</i> gene deletion of <i>P. chlororaphis</i> LDA-3	This work
LDA-5	<i>aroE</i> , <i>aroD</i> , <i>aroB</i> , <i>phzC</i> , <i>tktA</i> and <i>ppsA</i> overexpression in LDA-4	This work
Plasmids		
pEASY-Blunt	Blunt vector of gene cloning, Ap ^r , Kan ^r	Lab stock
pEASY-Blunt-aroD	Site mutant vector of <i>aroD</i>	This work
pEASY-Blunt-tktA	Site mutant vector of <i>tktA</i>	This work
pEASY-Blunt-ppsA	Site mutant vector of <i>ppsA</i>	This work
pK18mobsacB	Broad-host-range gene replacement vector, <i>sacB</i> , Kan ^r	Lab stock
pK18-phzF	vector for <i>phzF</i> deletion	This work
pK18-pykF	vector for <i>pykF</i> deletion	This work
pK18-rpeA	Vector for <i>rpeA</i> deletion	This work
pK18-psrA	Vector for <i>psrA</i> deletion	This work
pBbB5K-GFP	pBBR1; Kn ^r lacI P _{lac-UV5}	Lab stock
pBbB5K-aroE-aroD-aroB-phzC-tktA-ppsA	plasmid for <i>aroE</i> , <i>aroD</i> , <i>aroB</i> , <i>phzC</i> , <i>tktA</i> and <i>ppsA</i> , cooverexpression	This work

Table 1. Strains and plasmids used in this study.

BglBrick plasmids are a kind of widely used Brick plasmids¹⁷. The plasmid pBbB5K-GFP was used as the backbone to overexpress six key genes. Recombinant plasmids used in this study were constructed following the methods described in our previous research¹⁶. In brief, six Brick plasmids containing *aroB*, *aroD*, *aroE*, *phzC*, *tktA*, and *ppsA*, respectively, were first constructed. Point mutations were made in order to remove restriction sites (EcoRI, HindIII, BamHI, and BglII) in *aroD*, *tktA*, and *ppsA*. Then, a complicated overexpression plasmid pBbB5K-aroE-aroD-aroB-phzC-tktA-ppsA was constructed following the BglBrick standard.

Quantitative RT-PCR. Quantitative RT-PCR was used to detect the transcriptional changes of related genes of different strains. And the *rpoD* which is one of housekeeping gene in *P. chlororaphis* was selected as the internal reference gene. The measurement methods of Quantitative RT-PCR are following our previous work¹⁸. And the fold change for mRNAs was calculated by the $2^{-\Delta\Delta C_t}$ method¹⁹.

Fermentation processing. All *P. chlororaphis* strains were stored in an ultra-low temperature refrigerator. Strains were activated in KB petriplate with Ampicillin at 30 °C for 12–24 h before fermentation. Single colonies were inoculated in a 50 mL flask which contains 5 mL of KB medium and incubated overnight. Portions of seed bacteria were then inoculated in 50 mL KB medium in a 250 mL baffled flask and inoculation initial OD600 was 0.03. The gene expression of BglBrick plasmids was induced by isopropyl- β -D-thiogalactopyranoside (IPTG). 50 μ M IPTG was used during an incubation of 12 h. After growing at 30 °C and centrifuged at 200 rpm for 24–72 h, the fermentation broth was collected to measure phenazine compounds and OD600. All experiments were performed in triplicate, and data were averaged and reported as mean \pm standard deviation. After growing at 30 °C and 200 rpm for 24–72 h, the culture was collected for measurement of phenazine compounds and OD600. All fermentation experiments were performed in triplicate, and the data were averaged and reported as mean \pm standard deviation.

Measurement, purification, and quantification of DHHA from fermentation broth. Determination and purification of DHHA from fermentation broth followed the methods described in previous research²⁰. Briefly, the supernatant of the fermentation broth was collected by centrifuging at 12,000g for 15 min. Then, it was analyzed by liquid chromatography–mass spectrometry (LC–MS) after processing through a 0.22 μ m polyvinylidene difluoride syringe filter. LC–MS was performed on the Agilent HPLC1290-MS6230 system (Agilent Technologies, Santa Clara, CA) by an Agilent Extend C18 column (50 mm \times 2.1 mm, 1.8 μ m). It was eluted with methanol/0.1% formic acid (50:50, v/v) at a 0.15 mL/min flow rate. The DHHA sample was analyzed by mass spectrometry in the positive ion detection mode.

In order to purify DHHA, Shimadzu Inert Sustain phenyl column (20 \times 250 mm, 15 μ m) was used in HPLC (Shimadzu LC8A, Shimadzu, Kyoto, Japan). It was eluted with water/methanol (90:10, v/v) with a flow rate of

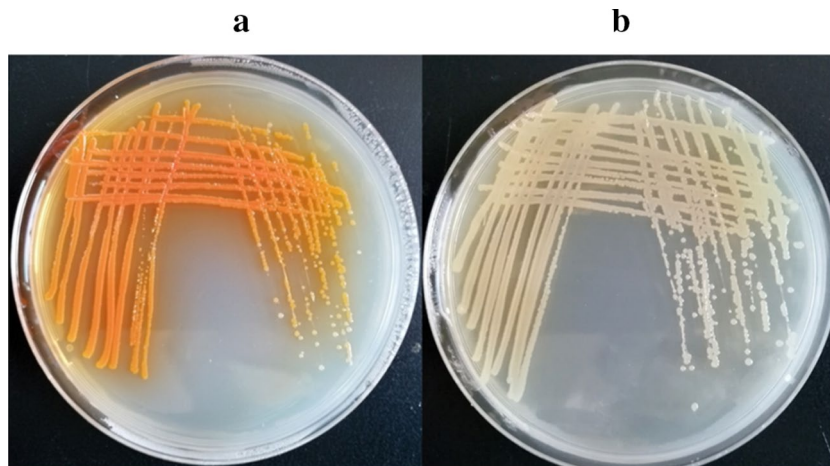


Figure 2. Colony morphology of *P. chlororaphis* Lzh-T5 and LDA-1. (a) Colony morphology of *P. chlororaphis* Lzh-T5. (b) Colony morphology of *P. chlororaphis* LDA-1.

2 mL/min at a scanning wavelength of 278 nm. We collected the peak containing DHHA and dried it by vacuum freezing. The crystals of DHHA were obtained at room temperature after dissolving them in hot ethanol (65 °C).

Quantification of DHHA was described in our previous work¹⁸. Briefly, the fermentation broth was centrifuged at 11,000 rpm for 3 min and supernatant collected. The samples were analysis by HPLC (Agilent 1260, USA) with a Shimadzu Inert Sustain phenyl column (4.6 × 250 mm, 5 μm) to determine the amount of DHHA. It was eluted with 0.1% formic acid/methanol (85:15, v/v) with a flow rate of 1 mL/min at a scanning wavelength of 278 nm. A DHHA standard curve was used to infer the DHHA content by plotting the concentration of the DHHA standard solution on the abscissa and the corresponding absorbance (peak area) on the vertical.

Superoxide dismutase activity measurement. In the Fe³⁺ addition experiments, superoxide dismutase (SOD) activities of different strains were measured. The methods of measure are following the previous literature^{21,22}.

Results

Disruption of phenazine synthesis in Lzh-T5. According to the research from Blankenfeldt, DHHA undergoes an isomerization reaction facilitated by PhzF and converts to 6-amino-5-oxocyclohex-2-ene-1-carboxylic acid in *Pseudomonas* spp²³. In order to accumulate DHHA, *phzF* was disrupted in *P. chlororaphis* Lzh-T5, and the strain *P. chlororaphis* LDA-1 was got. As shown in Fig. 2, after 48 h of culture, the *P. chlororaphis* LDA-1 strain on an agar plate turns milky; however, the colony color of Lzh-T5 remains orange. This suggests that the phenazine derivatives could not be synthesized in LDA-1. After fermentation and analysis by HPLC–UV, phenazines (including 2-hydroxyphenazine, PCA, and 2-OH-PCA) disappeared in the broth of *P. chlororaphis* LDA-1 (Fig. 3).

Similar to previous research, a new absorption peak appears in the HPLC–UV at a wavelength of 278 nm, which is the maximum absorption wavelength of DHHA (Fig. S1)²⁰. According to the analysis of LC–MS, the mass-to-charge ratio (m/z) of the compound was 156.0658 for [C⁷H₉NO₃⁺ H]⁺ (the mass of DHHA is 155.0655; Fig. S1). When *phzF* is overexpressed in the LDA-1 strain, production of phenazine was recovered (Fig. 3). According to these results, it suggests that disruption of *phzF* in Lzh-T5 causes accumulation of DHHA. Using HPLC–UV analysis, the DHHA yield of LDA-1 reached 2.15 g/L in 48 h (Fig. 4a). Our results suggest that disruption of *phzF* had little effect on Lzh-T5 cell growth (Fig. 4b).

Knockout of negative regulatory genes to boost DHHA production. According to previous research, interruption the *pykF* (which encode pyruvate kinase) enhances the production of 2-hydroxyphenazine¹⁶. In this study, *pykF* from LDA-1 was initially chosen to inactivate, so we obtained a mutant strain LDA-2 (Fig. 5). After analysis of the fermentation broth by HPLC–UV, the DHHA yield of strain LDA-2 increased from 2.15 g/L to 4.17 g/L (Fig. 5a). The growth condition of the strain was detected to have little effect after deletion of *pykF* (Fig. 5b).

PsrA, a sigma regulator, was first reported in *P. chlororaphis* PCL1391²⁴. According to Chin-A-Woeng et al., *PsrA* played a negative regulatory role in the production of the antifungal metabolite PCA in *P. chlororaphis* PCL1391²⁴. Similar results were obtained from *psrA* disruption in *P. chlororaphis* HT66 (Peng et al. 2018)²⁵. According to our research, the sigma regulator *psrA* also exists in *P. chlororaphis* Lzh-T5. The strain LDA-3 was obtained after the gene *psrA* was disrupted in LDA-2, and the production of DHHA increased from 4.17 g/L to 4.92 g/L (Fig. 5a).

RpeA, a negative regulator of Phenazine, was mutated by insertion in *P. chlororaphis* GP72 and results in a production increase of 2-hydroxyphenazine^{16,26}. *RpeA* is part of the two-component signal transduction system

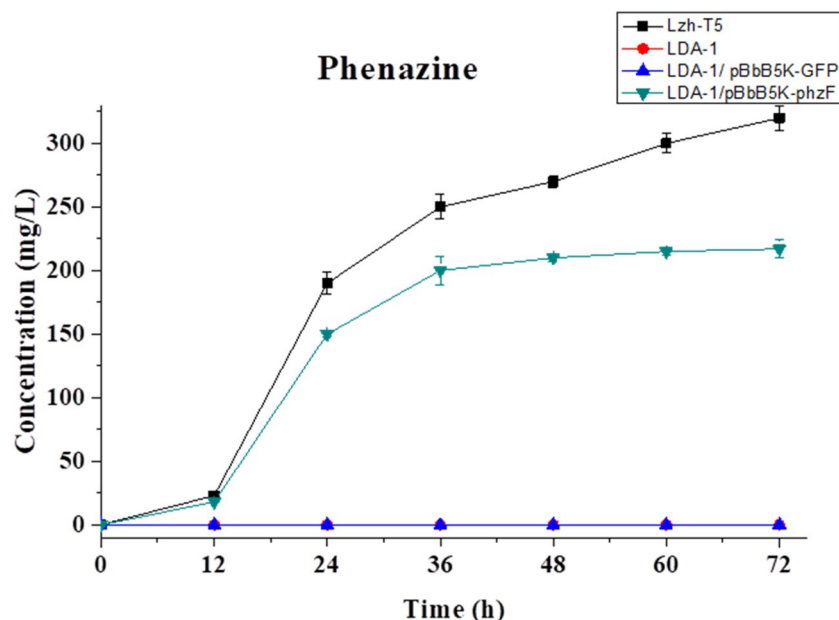


Figure 3. Phenazine production of *P. chlororaphis* Lzh-T5, LDA-1, LDA-1/pBbB5K-GFP, and LDA-1/pBbB5K-phzF.

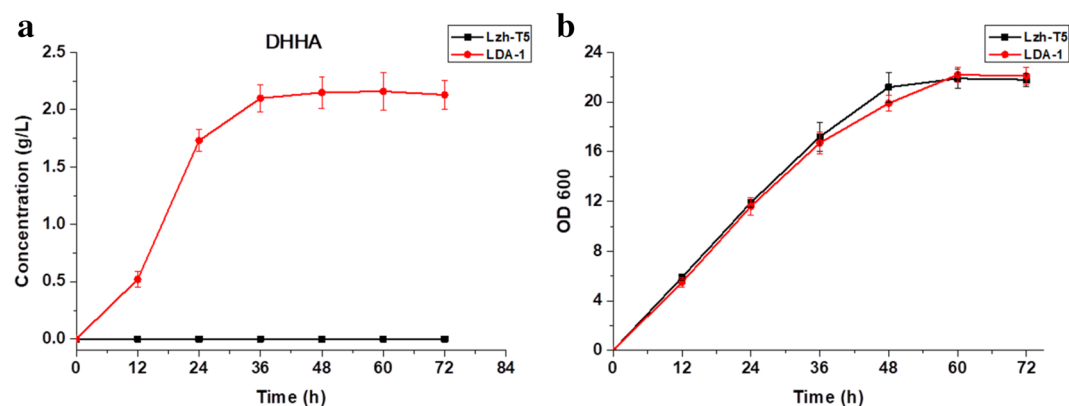


Figure 4. The DHHA production, growth curves of *P. chlororaphis* Lzh-T5 and LDA-1. (a) The DHHA production. (b) Growth curves.

(TCST) RpeA/RpeB, and is present in other *Pseudomonas* strains. For example, in *P. chlororaphis* 30–84, an RpeA homologue, negatively regulates the yield of PCA, indicating a conserved mechanism of *Pseudomonas* spp in phenazine synthesis regulation^{27,28}. In this study, *rpeA* was disrupted in the LDA-3 genome to construct LDA-4. Similar to the insertional mutagenesis of *P. chlororaphis* GP72, DHHA yield of LDA-4 increased from 4.92 g/L to 5.52 g/L (Fig. 5a). After knocking out the negative regulatory genes, quantitative RT-PCR results showed that the transcript level of genes *phzD* and *phzE* in the derivative strains, which is key gene for DHHA synthesis, has increased significantly (Fig. S2).

Enhanced DHHA production by key gene overexpression. We disrupted *pykF* to improve the yield of DHHA from 2.15 g/L to 4.17 g/L by diverting more metabolic flux into the shikimate pathway from other pathways (Fig. 5a). This indicates that enhancing the lead synthesis pathway, we could improve the yield of DHHA in *P. chlororaphis* Lzh-T5. Compared with knocking out negative regulatory genes, gene overexpression is another effective strategy often used to increase the yield of biologic products in microorganisms. According to previous research, overexpression of key genes in the shikimate pathway enhanced the yield of 2-OH-PHZ¹⁶. In order to increase the production of DHHA, *aroB*, *aroD*, *aroE*, *phzC*, *tktA*, and *ppsA* from Lzh-T5 were overexpressed from the shikimate, pentose phosphate, and gluconeogenesis pathways. We used a previously employed kind of modular vector, the BglBrick plasmid²⁹. A recombinant plasmid containing six genes, pBbB5K-aroE-aroD-aroB-phzC-tktA-ppsA, was constructed. Strain LDA-5 was created after transformation into the strain

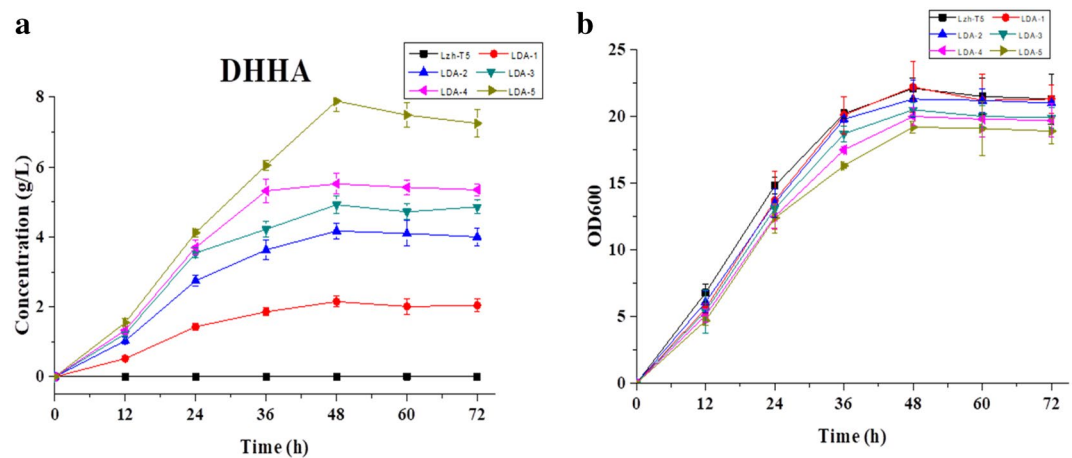


Figure 5. The DHHA production, growth curves of *P. chlororaphis* Lzh-T5, LDA-1, LDA-2, LDA-3, LDA-4, and LDA-5. (a) The DHHA production. (b) Growth curves.

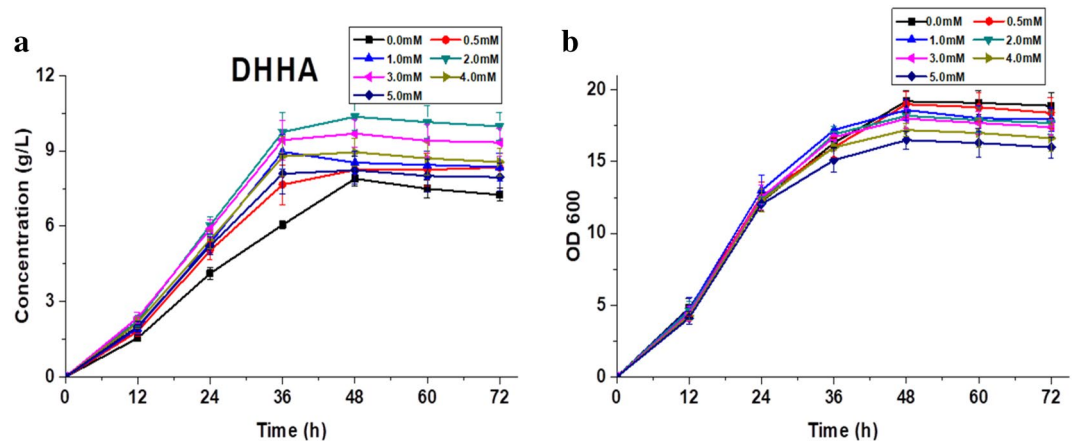


Figure 6. The DHHA production, growth curves of *P. chlororaphis* LDA-5 after different concentrations of Fe³⁺ adding. (a) The DHHA production and (b) growth curves.

LDA-4 by electrotransformation. After fermentation, the DHHA production of LDA-5 increased to 7.89 g/L after 48 h (Fig. 5a). This indicates that overexpression of key genes is an effective strategy to enhance the production of DHHA. Quantitative RT-PCR results showed that the transcript level of six genes overexpressed in the derivative strain LDA-5 has increased (Fig. S3).

Enhanced DHHA production with Fe³⁺. Environmental factors have important effects on secondary metabolite production in *Pseudomonas* strains, especial ion concentration in the medium^{30,31}. There is no universal medium suitable for *Pseudomonas* strains which can produce phenazines due to different nutritional requirements³⁰. According to previous research, the DHHA production has a 30% increase after adding 3 mM of Fe³⁺²⁰. To improve the production of DHHA, the effect of different concentrations of Fe³⁺ in the medium was investigated. After fermentation, DHHA production was detected by HPLC–UV. Low concentration of iron ions promoted DHHA production. High concentrations of iron ions inhibited DHHA production (Fig. 6). Different from our previous research, in the fermentation of LDA-5, the optimum concentration which enhanced the production of DHHA was 2 mM. We obtained a maximum DHHA yield of 10.45 g/L with 2 mM Fe³⁺ (Fig. 6a).

Discussion

Pseudomonas spp is a class of microorganism that exists widely in the environment³². It has strong adaptability and often produces resistant substances. Among these substances, phenazine derivatives are typical secondary metabolites, such as PCA, Pyocyanin (PYO), 2-Hydroxyphenazine and phenazine-1-carboxamide (PCN)^{25,33}. Phenazine derivatives are produced by the *phz* gene clusters (*phzABCDEF*) in several *Pseudomonas spp* (including *P. chlororaphis*, *P. fluorescens*, and *P. aeruginosa*)^{34–36}. In *P. chlororaphis*, *phzC* catalyzes the first reaction of the shikimic acid pathway, by catalysis of E4P and PEP to synthesize DAHP¹³. *PhzE*, the first key enzyme in the phenazine synthesis pathway which catalyzes the last product of the shikimate pathway into

2-amino-4-deoxy branched acid³⁷. ADIC converts to DHHA and pyruvate by the isobranse enzyme PhzD²³. It is then epimerized with diaminopimelate enzyme (diaminopimelate epimerase (DapF)) PhzF to 6-amino-5-oxocyclohex-2-ene-1-carboxylic acid (AOCHC)³⁸. Two molecules of AOCHC are converted to hexahydrophenazine-1,6-dicarboxylic acid (HHPDC) catalyzed by the dimer PhzAB²³. HHPDC spontaneously undergoes oxidative decarboxylation to form tetrahydrophenazine-1-carboxylic acid (THPCA). THPCA is catalyzed by PhzG to form 5,10-dihydro-phenazine-1-carboxylic acid (DHCCA)³⁹, DHCCA eventually undergoes self-oxidation in the air to form PCA. While DHHA is an important intermediate product of phenazines, the production of phenazines is quite low. For example, in wild type *P. chlororaphis* GP72, the yield of 2-OH-PHZ is 4.5 mg/L, and the higher phenazine (PCN) production in wild type is about 400 mg/L in *P. chlororaphis* HT66^{25,26}. The phenazine production strains are also the potential DHHA producers. *P. aeruginosa* is an opportunistic pathogenic bacterium, while *P. chlororaphis* is not. *P. chlororaphis* was selected as a candidate for DHHA production¹⁶. According to previous research, *P. chlororaphis* GP72 could accumulate 1.92 g/L DHHA with *phzF* disruption²⁰. Lzh-T5 is a *P. chlororaphis* strain isolated from the tomato rhizosphere found in China. It has the phenazine biosynthesis cluster *phzABCDEFG*, and can produce phenazine derivatives¹⁵. In this study, *phzF* was disrupted from the genome of *P. chlororaphis* Lzh-T5 making the strain *P. chlororaphis* LDA-1 which has 2.15 g/L DHHA accumulation.

Enhancing the shikimate pathway is an effective strategy for aromatic compound production in microorganisms²⁰. The direct precursors of the shikimate pathway are PEP and E4P. The PEP and E4P supply could be enhanced by an overexpression of PEP synthase encoded by *ppsA* and transketolase encoded by *tktA*^{1,40}. In addition, inactive *pykF*, which encodes pyruvate kinase, can increase PEP^{41,42}. Further carbon flux of the shikimate pathway impedes enzymatic reactions and removes the allosteric and transcriptional regions^{20,43}. Quinate/shikimate dehydrogenase, dehydroquinic acid synthase, dehydroquinic acid dehydratase, and DHAP synthetase, encoded by *aroE*, *aroB*, *aroD*, and *phzC*, respectively, were reported as limiting steps in the shikimate pathway⁴⁴. Our previous studies showed that disruption of pyruvate kinase (encoded by *pykF*) and coexpression of *ppsA*, *tktA*, *aroB*, *aroD*, *aroE*, and *phzC* in GP72 increased phenazine production²⁰. In this study, the disruption of *pykF* and six gene *tktA*, *ppsA*, *aroB*, *aroD*, *aroE*, and *phzC* coexpression in LDA-1 increased the DHHA production to 7.89 g/L.

TCST systems exist in *Pseudomonas spp* that help them adapt to the environment by coordinating cellular pathways to interact with the environment²⁸. Different TCST systems were found in *P. chlororaphis* Lzh-T5. Among these TCST systems, GacS/GacA is one of the most researched. GacS/GacA was the earliest TCST system which could enhance bioactive secondary metabolite production in *Pseudomonas spp*^{45,46}. In *P. chlororaphis* HT66, GacA positively regulates the expression of *psrA*. *psrA* negatively controls the expression of *rpoS* and the expression of phenazine²⁵. In this study, *psrA* was found in *P. chlororaphis* Lzh-T5. Interruption of *psrA* increased the production of DHHA from 4.17 g/L to 4.92 g/L, this suggests that *psrA* negatively controls the production of DHHA. RpeA/RpeB is a TCST system found widely in *Pseudomonas spp*²⁸. According to the research of Whistler et al., Pip improved the production of PCA by enhancing the expression of *phzR* and *phzI*. Sigma factor *rpoS* regulated the expression of *pip*, which itself is regulated by the RpeA/RpeB TCST system. RpeB was inhibited by RpeA, so an *rpeA* mutant strain enhanced the production of phenazine²⁸. Similar results were observed from *P. chlororaphis* GP72 and *P. chlororaphis* HT66^{16,25}. The *rpeA/rpeB* TCST system was found in *P. chlororaphis* Lzh-T5, interruption of *rpeA* results in the increase in DHHA from 4.92 g/L to 5.52 g/L (Fig. 5a). This result suggests that, similar with *P. chlororaphis* 30–84, *rpeA* negatively impacts the production of DHHA.

Metal ions are an important factor which could affect the production of secondary metabolites of *Pseudomonas spp*³⁰. Fe³⁺ is one of the important ions, and according to the research of Shtark et al., it plays a positive role in the production of phenazines in *P. chlororaphis* SPB1217. They hypothesize that Fe³⁺ activates some dependent superoxide dismutases and those superoxide dismutases promotes phenazine production by removing reactive oxygen species or bacterial metabolites that suppress enzymes involved in the synthesis pathway of phenazines³⁰. Similar results were reported in *P. aeruginosa* PCL1391 and *P. fluorescens* 2–79^{47,48}. Fe³⁺ also had a positive effect on DHHA production²⁰. And our results shown that the SOD activity of the strain has increased after Fe³⁺ adding to the medium (Fig. S4). In this study, adding different concentration of Fe³⁺ had different effects on DHHA production in *P. chlororaphis* LDA-5. Low concentrations of Fe³⁺ promoted DHHA production, while high concentrations of Fe³⁺ inhibited DHHA production (Fig. 6). Adding 2 mM of Fe³⁺ had a positive effect on DHHA production, and our maximum DHHA yield was 10.45 g/L in this study.

In conclusion, *phzF* of *P. chlororaphis* Lzh-T5 was disrupted to construct the strain *P. chlororaphis* LDA-1 which had DHHA accumulation. Then, three negative regulatory genes (*pykF*, *psrA* and *rpeA*) were disrupted stepwise in *P. chlororaphis* LDA-1. The production of DHHA increased from 2.15 g/L to 5.52 g/L. Next, different key genes selected from the shikimate, pentose phosphate, and gluconeogenesis pathways of Lzh-T5, were overexpressed by BglBrick vectors. The production of DHHA increased from 5.52 g/L to 7.89 g/L. The effect of adding Fe³⁺ on DHHA production was investigated in a strain (LDA-5) with a resulting DHHA yield of 10.45 g/L.

Data availability

All data generated or analyzed during this study are included in this published article (and its Additional file).

Received: 2 April 2021; Accepted: 8 July 2021

Published online: 12 August 2021

References

- Juaristi, E. & Soloshonok, V. *Enantioselective Synthesis of Beta-amino Acids* (Wiley, 2005).
- Bunnage, M. E., Ganesh, T., Masesane, I. B., Orton, D. & Steel, P. G. Asymmetric synthesis of the putative structure of (–)-oryzoxymycin. *Org. Lett.* 5(3), 239–242 (2003).
- Meade, T.J. Synthesis of aromatic heterocyclic polymers from a biosynthetically prepared precursor. *US Patent*. 5,340,913 (1994).

4. Palko, M., Kiss, L. & Fulop, F. Syntheses of hydroxylated cyclic beta-amino acid derivatives. *Curr. Med. Chem.* **12**(26), 3063–3083 (2005).
5. Lee, S. Y. *et al.* A comprehensive metabolic map for production of bio-based chemicals. *Nat. Catal.* **2**(1), 18–33 (2019).
6. Keasling, J. D. Manufacturing molecules through metabolic engineering. *Science* **330**(6009), 1355–1358 (2010).
7. Nielsen, J. Metabolic engineering. *Appl. Microbiol. Biotechnol.* **55**(3), 263–283 (2001).
8. Liu, Q. *et al.* Current state of aromatics production using yeast: Achievements and challenges. *Curr. Opin. Biotechnol.* **65**, 65–74 (2020).
9. Becker, J. *et al.* Top value platform chemicals: Bio-based production of organic acids. *Curr. Opin. Biotechnol.* **36**, 168–175 (2015).
10. Choi, S. *et al.* Biorefineries for the production of top building block chemicals and their derivatives. *Metab. Eng.* **28**, 223–239 (2015).
11. Noda, S. & Kondo, A. Recent advances in microbial production of aromatic chemicals and derivatives. *Trends Biotechnol.* **35**(8), 785–796 (2017).
12. McCormick, J. *et al.* (+) trans-2,3-dihydro-3-hydroxyanthranilic acid. A new amino acid produced by *Streptomyces aureofaciens*. *J. Am. Chem. Soc.* **83**, 4104–4105 (1961).
13. Mavrodi, D. V. *et al.* A seven-gene locus for synthesis of phenazine-1-carboxylic acid by *Pseudomonas fluorescens* 2–79. *J. Bacteriol.* **180**(9), 2541–2548 (1998).
14. McDonald, M. *et al.* Phenazine biosynthesis in *Pseudomonas fluorescens*: Branchpoint from the primary shikimate biosynthetic pathway and role of phenazine-1,6-dicarboxylic acid. *J. Am. Chem. Soc.* **123**(38), 9459–9460 (2001).
15. Li, Z. *et al.* Genome sequence of *Pseudomonas chlororaphis* Lzh-T5, a plant growth-promoting rhizobacterium with antimicrobial activity. *Genome Announc.* **6**(18), e00328 (2018).
16. Liu, K. *et al.* Genetic engineering of *Pseudomonas chlororaphis* GP72 for the enhanced production of 2-Hydroxyphenazine. *Microb. Cell Fact.* **15**(1), 131 (2016).
17. Li, Q. A. *et al.* Ligand binding induces an ammonia channel in 2-amino-2-desoxyisochorismate (ADIC) synthase PhzE. *J. Biol. Chem.* **286**(20), 18213–18221 (2011).
18. Jin, X. J. *et al.* iTRAQ-based quantitative proteomic analysis reveals potential factors associated with the enhancement of phenazine-1-carboxamide production in *Pseudomonas chlororaphis* P3. *Sci. Rep.* **6**, 27393 (2016).
19. Livak, K. J. & Schmittgen, T. D. Analysis of relative gene expression data using real-time quantitative PCR and the 2^{-ΔΔCT} method. *Methods* **25**, 402–408 (2001).
20. Hu, H. *et al.* Production of trans-2,3-dihydro-3-hydroxyanthranilic acid by engineered *Pseudomonas chlororaphis* GP72. *Appl. Microbiol. Biotechnol.* **101**(17), 6607–6613 (2017).
21. Weydert, C. J. & Cullen, J. J. Measurement of superoxide dismutase, catalase and glutathione peroxidase in cultured cells and tissue. *Nat. Protoc.* **5**, 51–66 (2010).
22. Martins, D. *et al.* Superoxide dismutase activity confers (p)ppGpp-mediated antibiotic tolerance to stationary-phase *Pseudomonas aeruginosa*. *Proc. Natl. Acad. Sci. U. S. A.* **115**, 9797–9802 (2018).
23. Blankenfeldt, W. *et al.* Structure and function of the phenazine biosynthetic protein PhzF from *Pseudomonas fluorescens*. *Proc. Natl. Acad. Sci. U. S. A.* **101**(47), 16431–16436 (2004).
24. Chin, A. W. T. F. *et al.* The *Pseudomonas chlororaphis* PCL1391 sigma regulator psrA represses the production of the antifungal metabolite phenazine-1-carboxamide. *Mol. Plant Microbe Interact.* **18**(3), 244–253 (2005).
25. Peng, H. *et al.* Enhanced biosynthesis of phenazine-1-carboxamide by engineered *Pseudomonas chlororaphis* HT66. *Microb. Cell Fact.* **17**(1), 117 (2018).
26. Huang, L. *et al.* Enhanced production of 2-hydroxyphenazine in *Pseudomonas chlororaphis* GP72. *Appl. Microbiol. Biotechnol.* **89**(1), 169–177 (2011).
27. Wang, D. *et al.* Differential regulation of phenazine biosynthesis by RpeA and RpeB in *Pseudomonas chlororaphis* 30–84. *Microbiology* **158**(Pt 7), 1745–1757 (2012).
28. Whistler, C. A. & Pierson, L. S. 3rd. Repression of phenazine antibiotic production in *Pseudomonas aureofaciens* strain 30–84 by RpeA. *J. Bacteriol.* **185**(13), 3718–3725 (2003).
29. Jumina, D. *et al.* Modular engineering of L-tyrosine production in *Escherichia coli*. *Appl. Environ. Microbiol.* **78**(1), 89–98 (2012).
30. Shtark, O., Shaposhnikov, A. I. & Kravchenko, L. V. The production of antifungal metabolites by *Pseudomonas chlororaphis* grown on different nutrient sources. *Mikrobiologiya* **72**(5), 645–650 (2003).
31. Kerins, M. J. & Ooi, A. The roles of NRF2 in modulating cellular iron homeostasis. *Antioxid. Redox Signal.* **29**(17), 1756–1773 (2018).
32. Silby, M. W. *et al.* *Pseudomonas* genomes: Diverse and adaptable. *FEMS Microbiol. Rev.* **35**(4), 652–680 (2011).
33. Liu, H. *et al.* Characterization of a phenazine-producing strain *Pseudomonas chlororaphis* GP72 with broad-spectrum antifungal activity from green pepper rhizosphere. *Curr. Microbiol.* **54**(4), 302–306 (2007).
34. Shen, X. *et al.* Genome sequence of *Pseudomonas chlororaphis* GP72, a root-colonizing biocontrol strain. *J. Bacteriol.* **194**(5), 1269–1270 (2012).
35. Paulsen, I. T. *et al.* Complete genome sequence of the plant commensal *Pseudomonas fluorescens* Pf-5. *Nat. Biotechnol.* **23**(7), 873–878 (2005).
36. Nouwens, A. S. *et al.* Complementing genomics with proteomics: The membrane subproteome of *Pseudomonas aeruginosa* PAO1. *Electrophoresis* **21**(17), 3797–3809 (2000).
37. Lee, T. S. *et al.* BglBrick vectors and datasheets: A synthetic biology platform for gene expression. *J. Biol. Eng.* **5**, 12 (2011).
38. Parsons, J. F. *et al.* Structure and function of the phenazine biosynthesis protein PhzF from *Pseudomonas fluorescens* 2–79. *Biochemistry* **43**(39), 12427–12435 (2004).
39. Xu, N. *et al.* Trapped intermediates in crystals of the FMN-dependent oxidase PhzG provide insight into the final steps of phenazine biosynthesis. *Acta Crystallogr. D Biol. Crystallogr.* **69**(Pt 8), 1403–1413 (2013).
40. Jiang, M. & Zhang, H. Engineering the shikimate pathway for biosynthesis of molecules with pharmaceutical activities in *E. coli*. *Curr. Opin. Biotechnol.* **42**, 1–6 (2016).
41. Noda, S. *et al.* Metabolic design of a platform *Escherichia coli* strain producing various chorismate derivatives. *Metab. Eng.* **33**, 119–129 (2016).
42. Sengupta, S. *et al.* Metabolic engineering of a novel muconic acid biosynthesis pathway via 4-hydroxybenzoic acid in *Escherichia coli*. *Appl. Environ. Microbiol.* **81**(23), 8037–8043 (2015).
43. Gosset, G. Production of aromatic compounds in bacteria. *Curr. Opin. Biotechnol.* **20**(6), 651–658 (2009).
44. Kramer, M. *et al.* Metabolic engineering for microbial production of shikimic acid. *Metab. Eng.* **5**(4), 277–283 (2003).
45. Chancey, S. T. *et al.* Survival of GacS/GacA mutants of the biological control bacterium *Pseudomonas aureofaciens* 30–84 in the wheat rhizosphere. *Appl. Environ. Microbiol.* **68**(7), 3308–3314 (2002).
46. Heeb, S., Blumer, C. & Haas, D. Regulatory RNA as mediator in GacA/RsmA-dependent global control of exoproduct formation in *Pseudomonas fluorescens* CHA0. *J. Bacteriol.* **184**(4), 1046–1056 (2002).
47. Slininger, P. J. & Shea-Wilbur, M. A. Liquid-culture pH, temperature, and carbon (not nitrogen) source regulate phenazine productivity of the take-all biocontrol agent *Pseudomonas fluorescens* 2–79. *Appl. Microbiol. Biotechnol.* **43**(5), 794–800 (1995).
48. van Rij, E. T. *et al.* Influence of environmental conditions on the production of phenazine-1-carboxamide by *Pseudomonas chlororaphis* PCL1391. *Mol. Plant Microbe Interact.* **17**(5), 557–566 (2004).

Acknowledgements

This little article has been posted as a preprint on Research Square (www.researchsquare.com).

Author contributions

L.L. and W.W. conceived and designed the experiments. K.L. and W.Y. performed the experiments. Y.H., R.W., and P.L. analyzed the data. L.L. and K.L. drafted the manuscript. All authors have read and approved the final manuscript.

Funding

This work was financially supported by Focus on Research and Development Plan in Shandong Province (Nos. 2019JZZY011003, 2020CXGC010603); Shandong key project of Research & Development plan (No. 2019GSF107066); Young doctorate Cooperation Fund Project, Qilu University of Technology (Shandong Academy of Sciences) (No. BSHZ20180016); Natural Science Foundation of Shandong Province (Nos. ZR2019PC060, ZR2020QC044); Shandong Province Higher Educational Science and Technology Program (No. A18KA116); Open Project Program of State Key Laboratory of Biobased Material and Green Papermaking, Qilu University of Technology (No. KF201822). The funders had no role in study design, data collection and analysis, decision to publish, or preparation of the manuscript.

Competing interests

The authors declare no competing interests.

Additional information

Supplementary Information The online version contains supplementary material available at <https://doi.org/10.1038/s41598-021-94674-8>.

Correspondence and requests for materials should be addressed to L.L. or W.W.

Reprints and permissions information is available at www.nature.com/reprints.

Publisher's note Springer Nature remains neutral with regard to jurisdictional claims in published maps and institutional affiliations.



Open Access This article is licensed under a Creative Commons Attribution 4.0 International License, which permits use, sharing, adaptation, distribution and reproduction in any medium or format, as long as you give appropriate credit to the original author(s) and the source, provide a link to the Creative Commons licence, and indicate if changes were made. The images or other third party material in this article are included in the article's Creative Commons licence, unless indicated otherwise in a credit line to the material. If material is not included in the article's Creative Commons licence and your intended use is not permitted by statutory regulation or exceeds the permitted use, you will need to obtain permission directly from the copyright holder. To view a copy of this licence, visit <http://creativecommons.org/licenses/by/4.0/>.

© The Author(s) 2021